

and also somewhat higher than the observed value for free methyl radical. The predicted intensity is again higher by about 50% relative to the corresponding mode of free methyl radical. In **1b**, the most intense E symmetry mode, ν_7 , has only half of the intensity of the corresponding mode in **1a**.

Relative Energies at Lower Levels of Theory. It is noteworthy that very different results from those cited above are obtained at lower levels of theory (see Tables II and III). On the Born-Oppenheimer potential energy hypersurface at the HF/6-31G* level, the complex **1a** is lower in energy than the reactants by 1.36 kcal/mol. Including the ZPVE difference, **1a** becomes 0.14 kcal/mol higher than the reactants. Likewise, **1b** is not stable at the HF/6-31G* level after inclusion of ZPVE. The stabilities of both transition-state structure, **2a** and **2b**, are grossly underestimated at the Hartree-Fock level. At the MP2/6-31G* level, the reaction barriers are reasonably close to the G1 values, as are the heats of reaction.

Conclusions

The potential energy surfaces for the reactions $\text{CH}_3 + \text{HX} \rightarrow \text{CH}_4 + \text{X}$ ($\text{X} = \text{Cl}, \text{Br}$) in the vicinity of the transition state were

calculated at the G1 level of theory. Each reaction is found to proceed via a loosely hydrogen-bridged complex (**1a**, **1b**), of C_{3v} symmetry, which is formed without activation energy. At the G1 level, the complexes are lower in energy than reactants by 0.67 and 0.28 kcal/mol for $\text{CH}_3 + \text{HCl}$ and $\text{CH}_3 + \text{HBr}$ systems, respectively. The transition state (**2a**) for the $\text{CH}_3 + \text{HCl}$ reaction has energy 2.53 kcal/mol relative to the reactants, while for $\text{CH}_3 + \text{HBr}$ system the transition state (**2b**) is calculated to lie only 0.67 kcal/mol above reactants at the G1 level. Heats of reaction for the two reactions compared to experimental values at the same temperature (298 K) indicate that the error limits for G1 theory, 1.3 kcal/mol ($\text{X} = \text{Cl}$) and 2.2 kcal/mol ($\text{X} = \text{Br}$), are as found in previous applications.

Acknowledgment. The financial support of the Natural Sciences and Engineering Research Council of Canada is gratefully acknowledged. Y.C. thanks the University of Calgary for a Killam Scholarship. We also thank Academic Computer Services of the University of Calgary for a generous grant of computer time on the Convex C120.

Registry No. CH_3 , 2229-07-4; HCl, 7647-01-0; HBr, 10035-10-6.

Gas-Phase Generation and Characterization of Neutral and Ionized HSiOH, H₂SiO, H₂SiOH, and H₃SiO by Collisional-Activation and Neutralization-Reionization Mass Spectrometry

Ragampeta Srinivas,[†] Diethard K. Böhme,[‡] Detlev Sülzle, and Helmut Schwarz*

Institute for Organic Chemistry, Technical University Berlin, D-1000 Berlin 12, Germany

(Received: June 21, 1991; In Final Form: August 15, 1991)

Results of mass spectrometric measurements are reported which characterize the chemical bonding in the stable ions HSiOH^{++} , $\text{H}_2\text{SiO}^{++}$, H_2SiOH^+ , and H_3SiO^+ and provide evidence for the existence of the corresponding neutral molecules HSiOH, H_2SiO , H_2SiOH^* , and H_3SiO^* , in the gas phase. The experiments were performed with a modified four-sector ZAB mass spectrometer with a BEBE configuration and collision cells mounted in the intermediate field-free regions B(1)/E(1), E(1)/B(2), and B(2)/E(2). Observed collisional-activation (CA) mass spectra of the ions $[\text{H}_2\text{SiO}]^{++}$ and $[\text{H}_3\text{SiO}]^+$ generated from electron impact of tetramethoxysilane are most compatible with the connectivities HSiOH^{++} and H_2SiOH^+ , respectively. Neutralization-reionization (NRMS) experiments and CA experiments with the "recovery" signals established identical connectivities for the corresponding neutral species. Charge-reversal (CR) experiments with the negative ions $[\text{H}_2\text{SiO}]^{--}$ and $[\text{H}_3\text{SiO}]^-$ generated from $\text{C}_6\text{H}_5\text{SiH}_3$ by chemical ionization in the presence of N_2O were used to provide evidence for isomeric ions with the connectivities $\text{H}_2\text{SiO}^{++}$ and H_3SiO^+ while neutralization-reionization ("NR") experiments showed that the connectivities of the negative ions were carried forward to the corresponding neutral species. Theoretical predictions suggest that the H_3SiO^+ , which was observed experimentally, is in its triplet state.

I. Introduction

Silicon-containing molecules and ions of composition $[\text{Si}_n\text{O}_m\text{H}_n]$ with $n = 1-4$ have become the subject of considerable theoretical and experimental scrutiny. The interest in these species stems largely from the fields of ionospheric¹ and interstellar chemistry² and recent developments in thin silicon film plasma-deposition and etching technology.³⁻⁶

$[\text{Si}_n\text{O}_m\text{H}_n]$ has drawn the most attention, no doubt in part because of early interests in SiOH^+ as a sink for meteoric Si^+ ions in the earth's ionosphere¹ and as a source for interstellar SiO .² This interest has led to high-level calculations⁷ which, in concert with infrared laser spectroscopy experiments, culminated in the first spectroscopic observation of gas-phase SiOH^+ in the laboratory.⁸

Very recently in this laboratory, we have been able to demonstrate the existence of and characterize the chemical bonding of both the neutral isomers HSiO^* and SiOH^* and their ionic counterparts HSiO^+ and SiOH^+ using collisional-activation (CA) and neutralization-reionization mass spectrometry (NRMS) techniques.⁹

Our knowledge of the next two members of the series, i.e., neutral and ionic $[\text{Si}_2\text{O}_2\text{H}_2]$ and $[\text{Si}_2\text{O}_2\text{H}_3]$, is much less developed.

(1) Ferguson, E. E.; Fahey, D. W.; Fehsenfeld, F. C.; Albritton, D. L. *Planet. Space Sci.* **1975**, *23*, 1621.

(2) Turner, J. L.; Dalgarno, A. *Astrophys. J.* **1977**, *213*, 386.

(3) Powell, M. J.; Easton, B. C.; Hill, O. F. *Appl. Phys. Lett.* **1981**, *38*, 794.

(4) Meiners, L. G. *J. Vac. Sci. Technol.* **1982**, *21*, 655.

(5) Lucovsky, G.; Richard, P. D.; Tsu, D. V.; Lin, S. Y.; Markunas, R. J. *J. Vac. Sci. Technol.* **1986**, *A4*, 681.

(6) Kushner, M. J. *J. Appl. Phys.* **1988**, *63*, 2532.

(7) Botschwina, P.; Rosmus, P. *J. Chem. Phys.* **1985**, *82*, 1420.

(8) Warner, H.; Fox, A.; Amano, T.; Bohme, D. K. *J. Chem. Phys.* **1989**, *91*, 5310.

(9) Srinivas, R.; Sülzle, D.; Koch, W.; DePuy, C. H.; Schwarz, H. *J. Am. Chem. Soc.* **1991**, *113*, 5970.

* To whom correspondence should be addressed.

[†] On leave from the Indian Institute of Chemical Technology, Council of Scientific and Industrial Research, Hyderabad-500007 (A.P.), India.

[‡] On sabbatical leave from the Department of Chemistry and Centre for Research in Earth and Space Science, York University, North York, Ontario, Canada M3J 1P3.

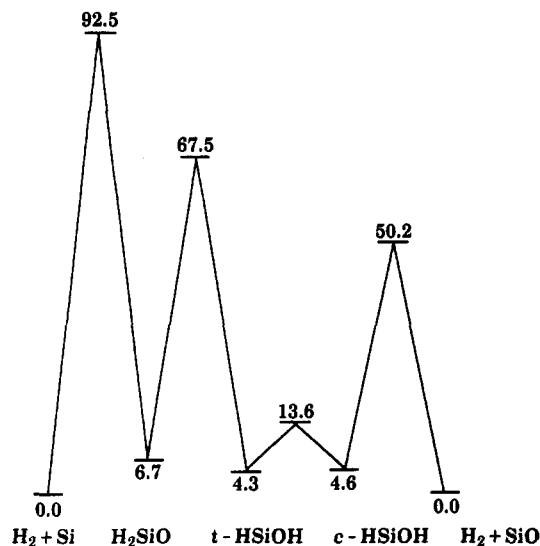


Figure 1. Potential energy diagram for $[\text{Si}, \text{O}, \text{H}_2]$ adapted from ref 10. Relative energies are in kilocalories per moles.

Apparently, with the exception of silanone, H_2SiO , neither neutral species has been shown to exist in the gas phase. Experimental evidence for silanone was provided first by infrared spectra recorded after irradiation of argon matrices containing silane and ozone.¹⁰ Chemiluminescent emission in the visible region produced by the oxidation processes in the gas-phase silane-ozone system also has been attributed to H_2SiO .¹¹ The infrared spectra of the *cis*- and *trans*- HSiOH (*c*- and *t*- HSiOH) isomers have been recorded in matrix isolation studies of the reaction of silicon atoms with water.¹² Interestingly, the *cis* isomer appeared to convert to the more stable *trans* isomer when the matrix was heated. High yields of HSiOH were also reported from the reaction of O atoms with silane promoted on an argon matrix.¹⁰

Quantum chemical calculations appear to be available only for neutral isomers of $[\text{Si}, \text{O}, \text{H}_2]$ ^{11,13-15} and ionic isomers of $[\text{Si}, \text{O}, \text{H}_3]^+$.¹⁶ Even silanol, H_3SiOH , an isomer of the fourth member of the series whose structure and properties have recently been calculated,¹⁷ has not yet been isolated or identified in the gas phase, although it has been observed as an intermediate in an infrared spectroscopic study of the oxidation of silane occurring in a solid argon matrix at 17 K.¹⁰

The three isomers of neutral $[\text{Si}, \text{O}, \text{H}_2]$, viz. silanone, H_2SiO , and the *cis* and *trans* isomers of hydroxysilylene, HSiOH , have been investigated in a comprehensive theoretical study by Kudo and Nagase.¹³ The results are summarized in Figure 1. The equilibrium structures of H_2SiO and *t*- HSiOH were calculated at the MP2/6-31G* level of theory while *c*- HSiOH and several transition structures were computed at the HF/6-31G* level. The HF/6-31G* structures were used to compute the total energies of the $[\text{Si}, \text{O}, \text{H}_2]$ species at several levels of theory. The significant results of these calculations regarding the isolation of the three isomers is that (at the CI(S+D+QC)/6-31G** level with all values corrected for zero-point vibrational energies), *t*- HSiOH is more stable than H_2SiO , but only by 2.4 kcal mol⁻¹, and the barrier for conversion of H_2SiO to *t*- HSiOH is as large as 60.8 kcal mol⁻¹. Other calculations for the energy difference between H_2SiO and *t*- HSiOH and for H_2SiO alone have appeared since but have not significantly changed the order of stability.^{11,14,15} The *cis* isomer is computed to be only 0.3 kcal mol⁻¹ less stable than

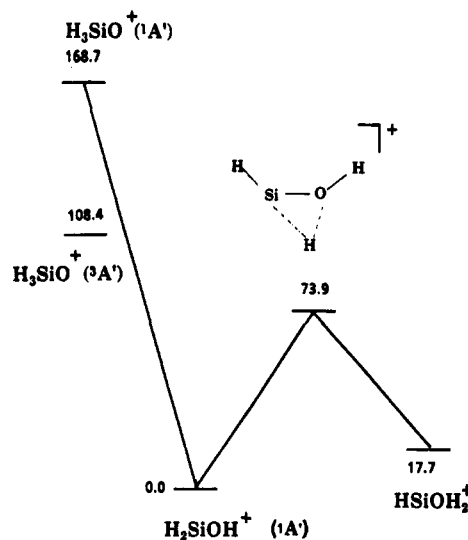


Figure 2. Potential energy diagram for $[\text{Si}, \text{O}, \text{H}_3]^+$ adapted from ref 14. Relative energies are in kilocalories per moles.

t- HSiOH , with a barrier of 9.0 kcal mol⁻¹ for its conversion to *t*- HSiOH .

Ab initio quantum chemical calculations have been reported for a number of isomers of $[\text{Si}, \text{O}, \text{H}_3]^+$.¹⁶ They are summarized in Figure 2. At the MP3/6-31G**//6-31G*+ZPC level of theory, H_2SiOH^+ has been found to be kinetically stable to a H 1,2-shift. While H_2SiOH^+ was calculated to be 17.7 kcal mol⁻¹ more stable than the 1,2-H-shifted isomer HSiOH_2^+ , the barrier for the H 1,2-shift was found to be 73.9 kcal mol⁻¹. The most stable conformation of H_2SiOH^+ is the fully planar structure with C_s symmetry. Both singlet and triplet states were examined for the Si-protonated cation H_3SiO^+ . The O-protonated cation was found to be much more stable at any level of theory than the Si-protonated cation. H_3SiO^+ ($^1A'$) and H_3SiO^+ ($^3A'$) are reported to be 168.7 and 108.4 kcal mol⁻¹, respectively, less stable than H_2SiOH^+ ($^1A'$). In addition, H_3SiO^+ ($^1A'$) was found to collapse to H_2SiOH^+ ($^1A'$) with no barrier so that the H_3SiO^+ species is likely to exist only in the triplet state.

There is an increasing need to understand species with composition $[\text{Si}, \text{O}, \text{H}_n]$, both neutral and ionic, as progress is being made rapidly in the characterization of their gas-phase chemistry. For example, recent studies of ion/molecule reactions of the π complexes $\text{Si}^{n+}/\text{benzene}$ and Si/Np^{n+} (Np = naphthalene) with H_2O suggest that $[\text{Si}, \text{O}, \text{H}_2]$ is formed as a neutral product, and it is interesting to know the connectivity of this species.^{18,19} Here we report the results of systematic CA and NRMS studies of ionic and neutral isomers with the elemental compositions $[\text{Si}, \text{O}, \text{H}_2]$ and $[\text{Si}, \text{O}, \text{H}_3]$, which may be derived by electron impact of tetramethoxysilane. The studies have revealed the existence in the gas phase of the stable neutral species HSiOH , H_2SiO , H_2SiOH^+ , and H_3SiO^+ and their respective ions.

II. Experimental Section

The experiments were performed with a substantially modified ZAB-HF mass spectrometer (V.G. Analytical Ltd., Wythenshawe, Manchester M23 9LE, U.K.), which is shown schematically in Figure 3. The mass spectrometer has four sectors with BEBE configuration where B denotes a magnetic and E denotes an electric sector. It was constructed by combining the BE part of an original ZAB-HF-3F BEB machine, denoted MS-1, with an AMD 604 double-focusing mass spectrometer of BE configuration (AMD Intectra GmbH, D-2833 Harpstedt, FRG), denoted as MS-2. MS-1 and MS-2 are coupled with a system of Einzel lenses.

Positive ions $[\text{Si}, \text{O}, \text{H}_2]^{n+}$ and $[\text{Si}, \text{O}, \text{H}_3]^+$ were generated by the ionization of tetramethoxysilane with 70-eV electrons. The

(10) Withnall, R.; Andrews, L. *J. Phys. Chem.* **1985**, *89*, 3261.

(11) Glinksi, R. J.; Gole, J. L.; Dixon, D. A. *J. Am. Chem. Soc.* **1985**, *107*, 5891.

(12) Ismail, Z. K.; Hauge, R. H.; Fredin, L.; Kauffman, J. W.; Margrave, J. L. *J. Chem. Phys.* **1982**, *77*, 1617.

(13) Kudo, T.; Nagase, S. *J. Phys. Chem.* **1984**, *88*, 2833.

(14) Tachibana, A.; Fueno, H.; Yamabe, T. *J. Am. Chem. Soc.* **1986**, *108*, 4346.

(15) Dixon, D. A.; Gole, J. L. *Chem. Phys. Lett.* **1986**, *125*, 179.

(16) Kudo, T.; Nagase, S. *Organometallics* **1986**, *5*, 1207.

(17) Sauer, J.; Ahlrichs, R. *J. Chem. Phys.* **1990**, *93*, 2575.

(18) Bohme, D. K. *Int. J. Mass Spectrom. Ion Proc.* **1990**, *100*, 719.

(19) Bohme, D. K.; Wlodek, S.; Wincel, H. *J. Am. Chem. Soc.* **1991**, *113*, 6396.

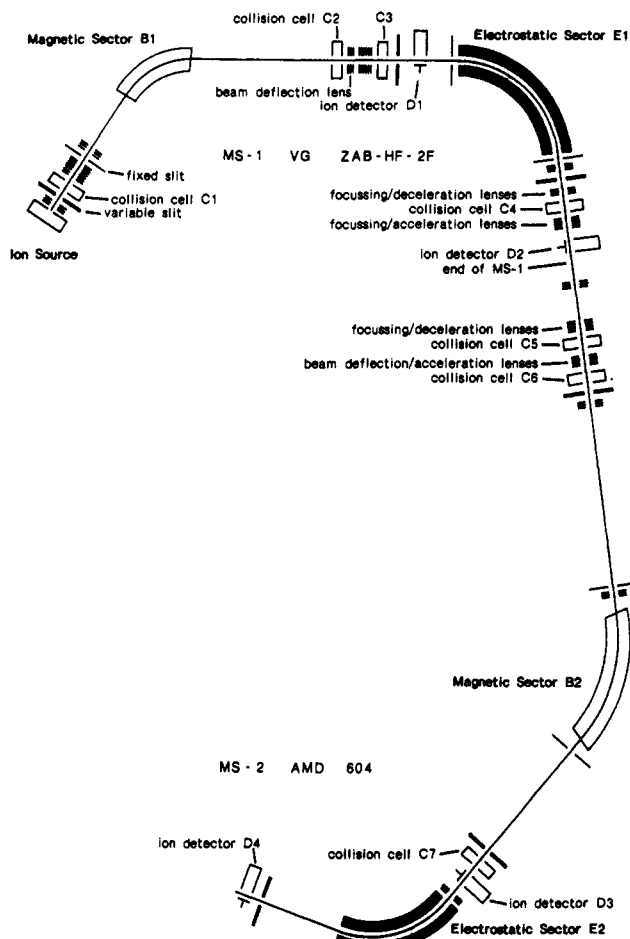


Figure 3. Schematic representation of the Berlin-BEBE tandem mass spectrometer (see text and ref 39 for details).

anions $[\text{Si}_2\text{O}_2\text{H}_2]^-$ and $[\text{Si}_2\text{O}_2\text{H}_3]^-$ were generated in the negative-ion mode (100-eV electrons) by chemical ionization at about 2×10^{-4} Torr using $\text{C}_6\text{H}_5\text{SiCH}_3$ as a precursor and N_2O as an electron-moderating gas and as a source of O^{*-} .²⁰ Otherwise, the ion-source conditions for both modes of operation were as follows: ion trap current in positive-ion mode, 100 μA ; emission current in chemical ionization mode, 500 μA ; ion-source temperature, 200 $^\circ\text{C}$; mass resolution $m/\Delta m = 1500$ (10% valley definition). For experiments with $[\text{Si}_2\text{O}_2\text{H}_3]^-$ the variable slits were fully open to obtain maximum signal intensities.

Collisional activation²¹⁻²⁵ used to characterize the ions leaving the source was achieved by mass-selecting the 8-keV ion beam by means of B(1)E(1) and colliding it, in the case of the positive ions, in collision chamber C6 located in the third field-free region (He, 80% transmittance, T). Ionic products were recorded by scanning B(2). Charge-reversal (CR) experiments^{22,23,26-28} were conducted by colliding the beam of mass-selected anions with oxygen (or helium, 80% T) also in the collision chamber C6 and recording the positively charged ions, along with ionic fragments derived thereof by scanning B(2). In the NRMS experiments²⁹⁻³⁵

(20) Gronert, S.; O'Hair, R. A. J.; Prodnuk, S.; Sulzle, D.; Damrauer, R.; DePuy, C. J. *Am. Chem. Soc.* **1990**, *112*, 997.

(21) Levsen, K.; Schwarz, H. *Angew. Chem., Int. Ed. Engl.* **1976**, *15*, 509.

(22) Cooks, R. G. Ed. *Collision Spectroscopy*; Plenum Press: New York, 1978.

(23) Levsen, K.; Schwarz, H. *Mass Spectrom. Rev.* **1985**, *3*, 77.

(24) Bordas-Nagy, J.; Jennings, K. R. *Int. J. Mass Spectrom. Ion Proc.* **1990**, *100*, 105.

(25) Cooks, R. G.; Ast, T.; Mabud, Md.A. *Int. J. Mass Spectrom. Ion Proc.* **1990**, *100*, 209.

(26) Beynon, J. H. *Proc. R. Soc. (London) Ser. A.* **1981**, *378*, 1.

(27) Bowie, J. H. *Mass Spectrom. Rev.* **1984**, *3*, 161.

(28) Bursey, M. M. *Mass Spectrom. Rev.* **1990**, *9*, 555.

(29) Terlouw, J. K.; Burgers, P. C.; v. Baar, B. L.; Weiske, T.; Schwarz, H. *Chimia* **1986**, *40*, 357.

(30) Wesdemiotis, C.; McLafferty, F. W. *Chem. Rev.* **1987**, *87*, 485.

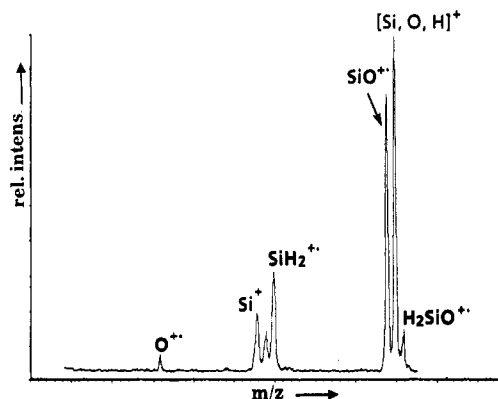


Figure 4. CR mass spectrum (He, 60% T) of m/z 46 $[\text{Si}_2\text{O}_2\text{H}_2]^+$ generated from $\text{C}_6\text{H}_5\text{SiH}_3$ with chemical ionization in the presence of N_2O .

the 8-keV beam of positive ions was neutralized with xenon (80% T) in the first cell, C5, of a differentially pumped tandem collision cell, C5/C6, located in the field-free region between E(1) and B(2). Unreacted ions were deflected away from the beam of neutral species by applying a voltage of 1000 V on the deflector electrode. Subsequent reionization occurred in the second collision cell, C6, by collision with oxygen (70% T). The resulting mass spectra were recorded by scanning B(2). The combination O_2/O_2 (80%, 80%) turned out to be most efficient for the CR/ NR^+ experiments³⁷ with $[\text{Si}_2\text{O}_2\text{H}_2]^+$ and $[\text{Si}_2\text{O}_2\text{H}_3]^+$. The minimum lifetime t (equal to the transit time from cell C5 to cell C6) is of the order of a microsecond.

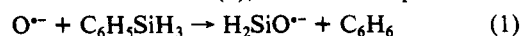
The availability of a multisector machine and the availability of collision cells in the field-free regions between B(1)/E(1) and E(1)/B(2) as well as B(2)/E(2) allowed further experiments for the positive ions which, on sensitivity grounds, could not be performed for $[\text{Si}_2\text{O}_2\text{H}_2]^+$ and $[\text{Si}_2\text{O}_2\text{H}_3]^+$. The positive ions $[\text{Si}_n\text{O}_n\text{H}_n]^+$ were mass-selected by B(1)E(1), neutralized with xenon (80% T), and reionized with oxygen (70% T) in the tandem collision cell located between E(1)/B(2). An interference-free beam of $[\text{Si}_n\text{O}_n\text{H}_n]^+$ was then selected with B(2) and subjected to collisional activation with helium (80% T). The CA mass spectrum was recorded by scanning E(2).

In all experiments, signal-averaging techniques were used to improve the S/N ratio. The data were accumulated by on-line processes using an AMD Intectra computer system DP 10.

III. Results and Discussion

Metastable decomposition experiments indicated several routes for the formation of the ions $[\text{Si}_2\text{O}_2\text{H}_2]^+$ and $[\text{Si}_2\text{O}_2\text{H}_3]^+$ from the molecular ion of tetramethoxysilane. The observed sequence of losses of CH_2O , CH_2O , CH_2O , and CH_4 is directly compatible with the formation of $[\text{Si}_2\text{O}_2\text{H}_2]^+$. Several routes leading to $[\text{Si}_2\text{O}_2\text{H}_3]^+$ were identified, and these involve the loss of CH_3^+ and three molecules of CH_2O in sequence in which the methyl radical is lost either first, second, third, or last.

A. $\text{H}_2\text{SiO}^+/\text{H}_2\text{SiO}$. Operation of the ion source in the negative-ion mode indicated the formation of $[\text{Si}_2\text{O}_2\text{H}_2]^-$ from phenylsilane and N_2O . A likely source for the formation of this ion is the ion-molecule reaction (1), which should produce the



H_2SiO^- isomer. The charge-reversal spectrum of this anion (Figure 4) shows two signals which are particularly structure indicative: m/z 30 (H_2Si^+) and m/z 16 (O^+). Also noteworthy are the absence of a signal at m/z 17 (OH^+), a relatively weak SiH^+ peak, and almost equal losses of $[\text{H}_2]$ and H^+ leading to SiO^+ and SiOH^+ , respectively. Clearly, this CR spectrum is

(31) Terlouw, J. K.; Schwarz, H. *Angew. Chem., Int. Ed. Engl.* **1987**, *26*, 805.

(32) Schwarz, H. *Pure Appl. Chem.* **1989**, *61*, 53.

(33) Holmes, J. L. *Adv. Mass Spectrom.* **1989**, *11*, 53.

(34) Holmes, J. L. *Mass Spectrom. Rev.* **1989**, *8*, 513.

(35) Terlouw, J. K. *Adv. Mass Spectrom.* **1989**, *11*, 984.

(36) McLafferty, F. W. *Science* **1990**, *247*, 925.

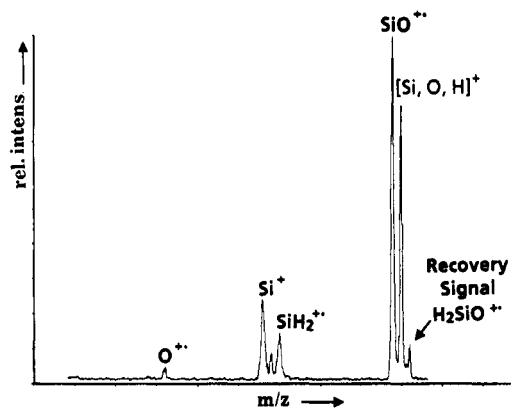


Figure 5. $\bar{\text{NR}}^+$ spectrum of $[\text{Si}_2\text{O}, \text{H}_2]^{++}$ generated from $[\text{Si}_2\text{O}, \text{H}_2]^-$ via CR (O_2 , 60% T ; He, 60% T). The total isotopic contribution of H^{29}SiO and ^{30}SiO to the recovery signal at m/z 46 is 7%.

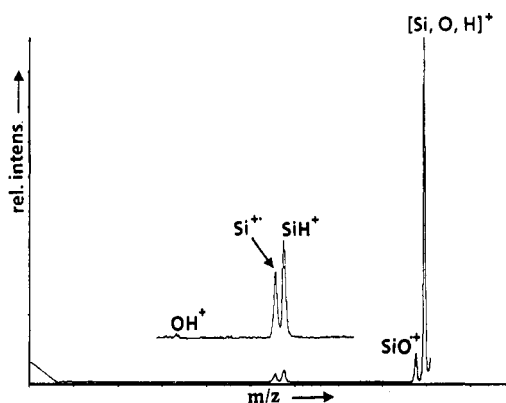
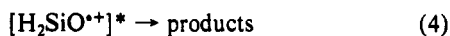
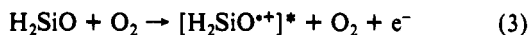
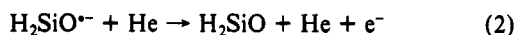


Figure 6. CA mass spectrum (He, 80% T) of m/z 46 $[\text{Si}_2\text{O}, \text{H}_2]^{++}$ generated from $\text{Si}(\text{CH}_3\text{O})_4$.

indicative of the production of a cation with the connectivity of silanone, viz. $\text{H}_2\text{SiO}^{++}$ rather than HSiOH^{++} .

The neutrals produced by electron detachment in the charge-reversal stage of H_2SiO^- were reionized to generate the positive-ion spectrum shown in Figure 5 according to the reaction sequence (2)–(4).



This so-called neutralization–reionization ($\bar{\text{NR}}^+$) spectrum, although less intense, is practically identical to the CR spectrum shown in Figure 4 and contains a fairly intense recovery signal (although not sufficiently large for further CA). We take this result as evidence for the intermediate formation of a neutral molecule with the connectivity H_2SiO .

B. $\text{HSiOH}^{++}/\text{HSiOH}$. The CA spectrum of the ion at m/z 46 produced directly from the tetramethoxysilane by electron impact and also corresponding to the elemental composition $[\text{Si}_2\text{O}, \text{H}_2]$ is shown in Figure 6. Intense fragment ions are observed at m/z 45 (SiOH^+), 44 (SiO^{++}), 29 (SiH^+), and 28 (Si^{++}) corresponding to loss of H^+ , $[\text{H}_2]$ (much weaker), $[\text{H}, \text{O}]$ and $[\text{H}_2, \text{O}]$, respectively, and a weak signal is evident at m/z 17 (OH^+) corresponding to loss of $[\text{H}, \text{Si}]$. The CA/CA spectrum of m/z 29 showed a loss of H, which indicates that some of this peak is SiH^+ and not $^{29}\text{Si}^{++}$. The peaks corresponding to SiH^+ and OH^+ observed in the CA spectrum and the weak loss of H_2 compared to H^+ are most compatible with the connectivity $\text{H}-\text{Si}-\text{OH}^{++}$ for the ion at m/z 46. Indeed, the CA spectrum in general is quite different from the CR spectrum in Figure 4 associated with the $\text{H}_2\text{SiO}^{++}$ isomer, which shows no OH^+ , a much smaller SiH^+ peak, and a loss of H_2 almost equal to the loss of H^+ . Also, the absence of signals at m/z 30 (SiH_2^{++}) and m/z 16 (O^{++}) rules out the contribution of any $\text{H}_2\text{SiO}^{++}$ isomer to the CA spectrum shown in Figure 6.

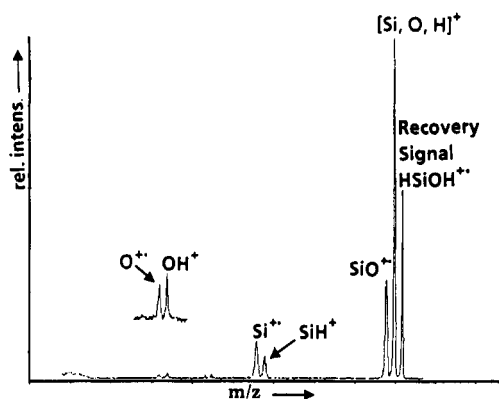


Figure 7. NR mass spectrum (Xe, 80% T ; O_2 , 70% T) of $[\text{Si}_2\text{O}, \text{H}_2]^{++}$. The total isotopic contribution of $\text{H}^{29}\text{SiO}^+$ and $^{30}\text{SiO}^+$ to the recovery signal at m/z 46 is 5.9%.

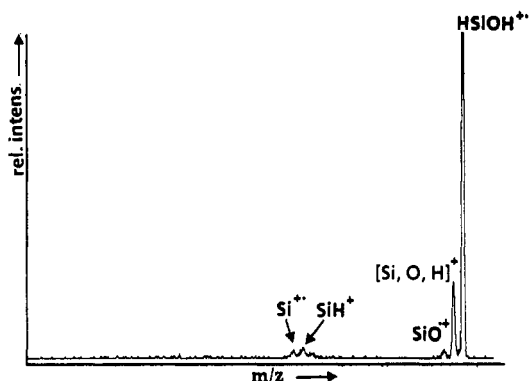
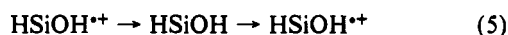


Figure 8. CA mass spectrum of reionized $[\text{Si}_2\text{O}, \text{H}_2]^{++}$: mass selection of m/z 46 with B(1)E(1); neutralization–reionization with Xe/ O_2 (80% T /70% T); selection of reionized m/e 46 with B(2) followed by collisional activation with He (80% T); energy analysis with E(2).

Figure 7 shows the abundant recovery signal which is observed when the m/z 46 ion is neutralized and reionized in a NRMS-type experiment. The observation of the recovery signal is consistent with nearly vertical neutralization and ionization processes as indicated in eq 5 so that the intermediate neutral species can be



assumed to have retained the connectivity of HSiOH^{++} and so to be given by HSiOH . The observed fragmentation pattern shown in Figure 7 is consistent with this connectivity (the new peak at m/z 16 may be attributed to O^{++} produced from the collisional dissociative ionization of OH produced in the neutralization step). The interference-free CA mass spectrum for the reionized HSiOH species given in Figure 8, although less intense, shows the same diagnostic peaks observed in the CA spectrum of the initial m/z 46 ion shown in Figure 6. Given the knowledge that the $\bar{\text{NR}}^+$ spectrum of the $\text{H}_2\text{SiO}^{++}$ isomer is significantly different, we may conclude from this result that no substantial interconversion has occurred in the neutralization–reionization sequence given by eq 5. The assignment made for the connectivity of the neutral molecule, HSiOH , is consistent with that predicted for the ground state of this species.

C. $\text{H}_2\text{SiOH}^+/\text{H}_2\text{SiOH}^+$. The CA spectrum of the m/z 47 ion generated from tetramethoxysilane by electron impact and with the elemental composition $[\text{Si}_2\text{O}, \text{H}_3]$ is shown in Figure 9.

The base peak, corresponding to elimination of $[\text{H}_2]$, lies at m/z 45 $[\text{Si}, \text{O}, \text{H}]^+$ between two weaker peaks at m/z 46 $[\text{Si}_2\text{O}, \text{H}_2]^{++}$ and m/z 44 (SiO^{++}) corresponding to loss of H and $[\text{H}_3]$, respectively. Other peaks are found at m/z 30 (H_2Si^{++}), 29 (HSi^+), and 28 (Si^{++}) corresponding to loss of $[\text{H}, \text{O}]$, $[\text{H}_2, \text{O}]$, and $[\text{H}_3, \text{O}]$, respectively, and, although with much less intensity, at m/z 17 (OH^+) and 16 (O^{++}) corresponding to loss of $[\text{H}_2, \text{Si}]$ and $[\text{H}_3, \text{Si}]$, respectively. The structure-indicative group of signals at m/z 28–30 and the signal at m/z 17 suggest the connectivity H_2SiOH^+ . No peak was observed at m/z 31 (SiH_3^+), which would be in-

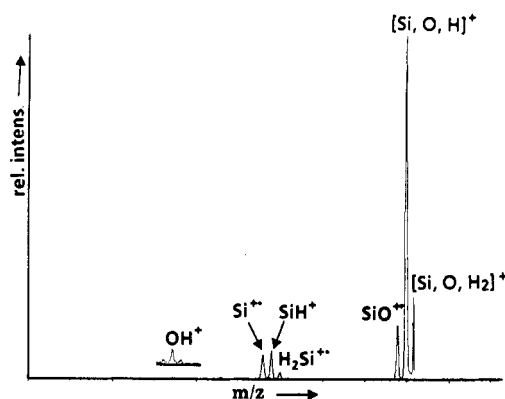


Figure 9. CA mass spectrum (He, 80% *T*) of *m/z* 47 [Si, O, H₃]⁺ generated from Si(CH₃O)₄.

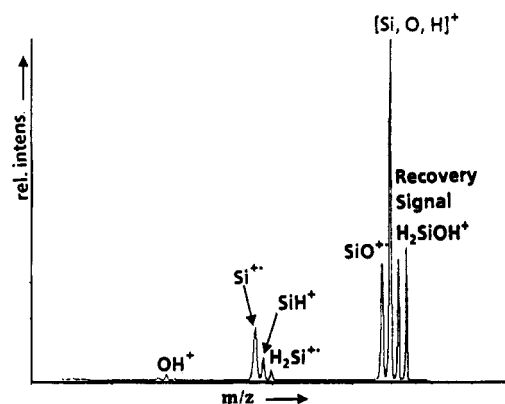
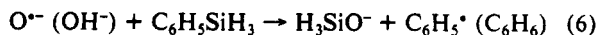


Figure 10. NR mass spectrum (Xe, 80% *T*; O₂, 80% *T*) of [Si, O, H₃]⁺. The total isotopic contribution of H₂²⁹SiO⁺ and H³⁰SiO⁺ to the recovery signal at *m/z* 47 is 6.0%.

dicative of a connectivity of the type H₃SiO⁺. The very small peak at *m/z* 18 (OH₂⁺⁺) may be indicative of trace amounts of an isomer of the connectivity HSiOH₂⁺ either present in the original beam or formed by collision-induced isomerization. Neutralization of *m/z* 47 followed by reionization again yielded an intense recovery signal in addition to the structurally diagnostic ions at *m/z* 28, 29, 30, and 17 as shown in Figure 10. So, we can conclude again that the neutral intermediate has the same connectivity as the ion at *m/z* 47, i.e., the connectivity H₂SiOH⁺. The multistep collision experiment gives rise to the interference-free CA spectrum of the reionized H₂SiOH⁺ shown in Figure 11 which, although less intense, matches the CA spectrum of the initial *m/z* 47 ion perfectly so that it may again be argued that no substantial interconversion occurs in the sequential neutralization–reionization collisions.

The assignments made for the connectivities of the ion H₂SiOH⁺ and the neutral molecule H₂SiOH⁺ should again correspond to those expected for the ground states of these species. Unfortunately, no information, theoretical or experimental, is available for the neutral species to provide further insight. However, the calculations summarized in Figure 2 predict the same connectivity for the ground state of the H₂SiOH⁺ ion which we have assigned.¹⁶

D. H₃SiO⁺/H₃SiO⁺. The possibility of generating the triplet H₃SiO⁺ ion indicated by theory¹⁶ is intriguing (see Figure 2). Indeed, our experimental results suggest that we have made this ion. Operation in the negative-ion mode indicated that a second isomeric ion at *m/z* 47 [Si, O, H₃]⁻ could be generated by charge reversal of an anion at *m/z* 47 [Si, O, H₃]⁻ generated from phenylsilane and N₂O. The source of the *m/z* 47 anion is likely to be the ion/molecule reaction with O⁻, reaction 6, and, to a lesser



extent, OH⁻, and it should therefore have the connectivity H₃-SiO⁻.²⁸ The charge-reversal spectrum of the *m/z* 47 cation produced from the *m/z* 47 anion using either O₂ or He as the

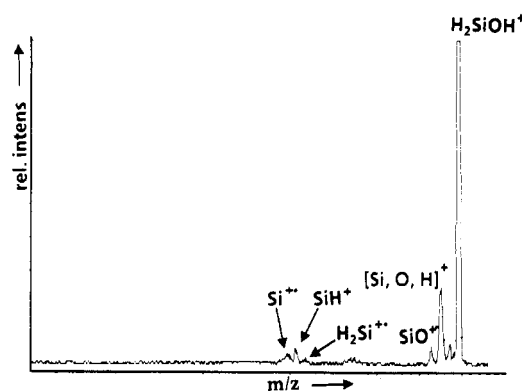


Figure 11. CA mass spectrum of reionized [Si, O, H₃]⁺⁺: mass selection of *m/z* 47 with B(1)E(1); neutralization–reionization with Xe/O₂ (80% *T*/80% *T*); selection of reionized *m/z* 47 with B(2), followed by collisional activation with He (80% *T*); energy analysis with E(2).

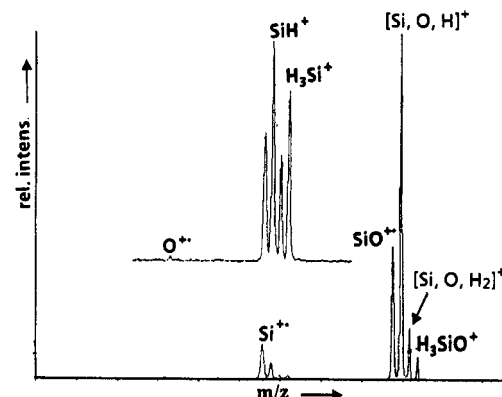
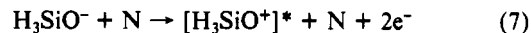


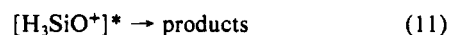
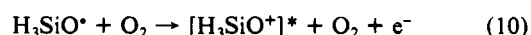
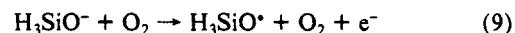
Figure 12. CR mass spectrum (O₂, 80% *T*) of *m/z* 47 [Si, O, H₃]⁻ generated from C₆H₅SiH₃ with chemical ionization in the presence of N₂O. Inset shows CR mass spectrum using He (80% *T*).

charge-reversal gas as illustrated by reactions 7 and 8 (with N = O₂ or He) is shown in Figure 12.



With the structurally diagnostic signals at *m/z* 28 (Si⁺⁺), 29 (HSi⁺⁺), 30 (H₂Si⁺⁺), and in particular 31 (H₃Si⁺⁺) and the weak signal at *m/z* 16 (O⁺⁺), the CR spectrum is most compatible with the connectivity H₃SiO⁺ rather than H₂SiOH⁺. The differences in relative peak heights observed with helium (see inset) can be attributed to a higher excitation with helium collision gas so that the more endothermic decomposition channels become more accessible.^{28,37} Given that the singlet state of H₃SiO⁺ should isomerize to the singlet H₂SiOH⁺ ion¹⁴ and the incompatibility of the observed CR spectrum with the connectivity H₂SiOH⁺, we can conclude that reaction 7 establishes the triplet state of H₃SiO⁺ in a manner quite analogous to the production of the triplet state of H₃CO⁺.³⁸ It may also be noted that the singlet H₃SiO⁺ may isomerize to HSiOH₂⁺ since this process is exothermic and that such an isomerization may account for the trace amounts of HSiOH₂⁺ which seem to have been observed.

The neutral molecules produced by electron detachment in the charge-reversal stage of H₃SiO⁻ were reionized to generate the positive-ion spectrum shown in Figure 13 according to the reaction sequence (9)–(11). This –NR⁺ spectrum, although less intense,



(37) Mercer, R. S.; Harrison, A. G. *Org. Mass Spectrom.* **1987**, *22*, 710.
 (38) Burgers, P. C.; Holmes, J. L. *Org. Mass Spectrom.* **1984**, *19*, 452.
 (39) Srinivas, R.; Sülzle, D.; Weiske, T.; Schwarz, H. *Int. J. Mass Spectrom. Ion Proc.* **1991**, *107*, 369.

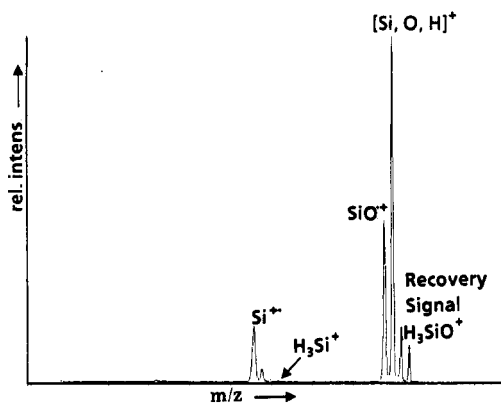


Figure 13. $^{-}\text{NR}^{+}$ spectrum of $[\text{Si}, \text{O}, \text{H}_3]^{+}$ generated from $[\text{Si}, \text{O}, \text{H}_3]^{-}$ via CR (O_2 , 80% T; O_2 , 80% T).

is practically identical to the CR spectrum shown in Figure 12 and contains a fairly intense recovery signal (although again not sufficiently large for further CA). We take this as evidence for the intermediate formation of a neutral molecule with the connectivity $\text{H}_3\text{SiO}^{\bullet}$.

IV. Conclusions

1. Collisional activation experiments have established the

connectivities HSiOH^{+} and $\text{H}_2\text{SiOH}^{+}$ for the ions at m/z 46 and 47 generated by electron impact of tetramethoxysilane.

2. Neutralization-reionization experiments have established the connectivities HSiOH and $\text{H}_2\text{SiOH}^{\bullet}$ for the neutral species derived from HSiOH^{+} and $\text{H}_2\text{SiOH}^{+}$ by neutralization at high collision energies. The connectivity for HSiOH is the same as that predicted by theory for the ground state of this molecule.

3. Charge-reversal experiments with H_2SiO^{-} and H_3SiO^{-} have established the connectivities H_2SiO^{+} and H_3SiO^{+} . Theoretical predictions suggest that the H_3SiO^{+} ion produced by charge reversal of the siloxide anion is the higher energy isomer and that this ion must be in its triplet state.

4. Neutralization-reionization experiments have provided evidence for the stability of the neutral molecules H_2SiO and $\text{H}_3\text{SiO}^{\bullet}$.

Acknowledgment. Financial support of our work by the Deutsche Forschungsgemeinschaft and the Fonds der Chemischen Industrie is appreciated. R.S. acknowledges the receipt of a visiting fellowship from the Deutscher Akademischer Austauschdienst (DAAD) and the encouragement of Dr. A. V. Rama Rao, Director, ICT, Hyderabad (India). D.K.B. is grateful to the Alexander-von-Humboldt Foundation for a Humboldt Senior Scientist Award and to Professor H. Schwarz for his hospitality. We are indebted to Dr. Thomas Weiske for technical assistance.

Reaction Kinetics of Coordinatively Unsaturated Iron Carbonyls Formed on Gas-Phase Excimer Laser Photolysis of $\text{Fe}(\text{CO})_5$

Robert J. Ryther and Eric Weitz*

Department of Chemistry, Northwestern University, Evanston, Illinois 60208-3113
(Received: December 27, 1990; In Final Form: July 8, 1991)

The reactions of species produced on gas-phase excimer laser photolysis of $\text{Fe}(\text{CO})_5$ have been followed by transient infrared spectroscopy employing a diode laser probe. The initial photoproducts formed on 193-nm photolysis are identified as $\text{Fe}(\text{CO})_2$ and a product that is most likely $\text{Fe}(\text{CO})$. Both $\text{Fe}(\text{CO})_2$ and $\text{Fe}(\text{CO})_3$ are produced on 248-nm photolysis. Photolysis at 351 nm leads to the production of both $\text{Fe}(\text{CO})_3$ and $\text{Fe}(\text{CO})_4$. Species best assigned as excited states of $\text{Fe}(\text{CO})_3$ and $\text{Fe}(\text{CO})_4$ are observed to form as initial photoproducts following 248- and 351-nm photolysis, respectively. The magnitudes of the rate constants for reaction of the various coordinatively unsaturated metal carbonyls formed in this study with parent $\text{Fe}(\text{CO})_5$ or CO (summarized in Table I) are consistent with the hypothesis that spin-allowed reactions will be rapid while spin-disallowed reactions will be considerably slower. To provide further data in testing this hypothesis, the reaction of $\text{Fe}(\text{CO})_4$ with both O_2 and H_2 has been measured.

I. Introduction

Studies of metal carbonyl photochemistry have provided a wealth of information on the photochemistry, photophysics, and reactive behavior of coordinatively unsaturated species.¹⁻¹⁵ A

particularly well-studied and important metal carbonyl is $\text{Fe}(\text{CO})_5$. It has been shown that photolysis of $\text{Fe}(\text{CO})_5$ can lead to the production of active catalytic species for olefin hydrogenation,¹⁻³ hydrosilation,⁴⁻⁷ and isomerization^{2,3,8,9} reactions. Gas-phase, UV photolysis of $\text{Fe}(\text{CO})_5$ has been used for deposition of thin films of metal on semiconductor or magnetic memory storage devices^{10,11} and for deposition of iron carbonyl catalysts on surfaces.^{5-7,12,13} Similarities between metal carbonyls and carbon monoxide bound to metal surfaces also aid in modeling of surface-molecule interactions¹² which can be used in interpreting both theoretical and experimental surface science studies.

Applications of transient infrared spectroscopy to the study of coordinatively unsaturated metal carbonyls is relatively recent, but it is already clear that this technique has revealed a number of new and interesting features regarding the photochemistry and reactive behavior of these species.¹⁵ Though almost all the coordinatively unsaturated metal carbonyls that have been studied to date react very rapidly with CO and the parent carbonyl, $\text{Fe}(\text{CO})_4$ is an anomaly. Its rate constant for reaction with CO

- (1) Whetten, R. L.; Fu, K. J.; Grant, E. R. *J. Chem. Phys.* **1982**, *77*, 3769.
- (2) Wrighton, M. S.; Ginley, D. S.; Schroeder, M. A.; Morse, D. L. *Pure Appl. Chem.* **1975**, *41*, 671.
- (3) Schroeder, M. A.; Wrighton, M. S. *J. Am. Chem. Soc.* **1976**, *98*, 551.
- (4) Mitchener, J. C.; Wrighton, M. S. *J. Am. Chem. Soc.* **1981**, *103*, 975.
- (5) Trusheim, M. R.; Jackson, R. L. *J. Phys. Chem.* **1983**, *87*, 1910.
- (6) Jackson, R. L.; Trusheim, M. R. *J. Am. Chem. Soc.* **1982**, *104*, 6590.
- (7) Darsillo, M. S.; Gafney, H. D.; Paquette, M. S. *J. Am. Chem. Soc.* **1987**, *109*, 3275.
- (8) Whetten, R. L.; Fu, K. J.; Grant, E. R. *J. Am. Chem. Soc.* **1982**, *104*, 4270.
- (9) Weiller, B. H.; Grant, E. R. *J. Am. Chem. Soc.* **1987**, *109*, 1051.
- (10) Kompa, K. L. *Angew. Chem., Int. Ed. Engl.* **1988**, *27*, 1314.
- (11) Schröder, H.; Kompa, K. L.; Masci, D.; Gianinoni, I. *Appl. Phys.* **1985**, *A38*, 227.
- (12) Plummer, E. W.; Salaneck, W. R.; Miller, J. S. *Phys. Rev. B* **1978**, *18*, 1673.
- (13) Swanson, J. R.; Friend, C. M.; Chabal, Y. J. *J. Chem. Phys.* **1987**, *87*, 5028.
- (14) Barton, T. J.; Grinter, R.; Thomson, A. J.; Davies, B.; Poliakov, M. *J. Chem. Soc., Chem. Commun.* **1977**, 841.

- (15) Poliakov, M.; Weitz, E. *Adv. Organometallic Chem.* **1986**, *25*, 277. *Acc. Chem. Res.* **1987**, *20*, 408.